Histol Histopathol (2024) 39: 1025-1035

Histology and Histopathology
From Cell Biology to Tissue Engineering

ORIGINAL ARTICLE Open Access

Identification and validation of plasma AGRN as a novel diagnostic biomarker of hepatitis B Virus-related chronic hepatitis and liver fibrosis/cirrhosis

Rong Ai[1,2]*, Lu Li[1,2]*, Xiwei Yuan[1,2], Dandan Zhao[1,2], Tongguo Miao[1,2], Weiwei Guan[1,2], Shiming Dong[1,2], Chen Dong[1,2], Yao Dou[1,2], Mengmeng Hou[1,2] and Yuemin Nan[1,2]

[1]Department of Traditional and Western Medical Hepatology, Third Hospital of Hebei Medical University and [2]Hebei Provincial Key Laboratory of Liver Fibrosis in Chronic Liver Diseases, Shijiazhuang, China

*These authors contributed equally to this work

Summary. Objective. The aim of this study was to find novel biomarkers and develop a non-invasive, effective diagnostic model for hepatitis B Virus-related chronic hepatitis and liver fibrosis/cirrhosis.

Method. Quantitative real-time polymerase chain reaction (qRT-PCR) was utilized to assess the expression of differentially expressed genes (*AGRN*, *JAG1*, *CCL5*, *ID3*, *CCND1*, and *CAPN2*) in peripheral blood mononuclear cells (PBMCs) from healthy subjects, chronic hepatitis B (CHB), and liver fibrosis/cirrhosis (LF/LC) patients. The molecular mechanisms underlying AGRN-regulated CHB were further explored and verified in LX2 cells, in which small interfering RNA (siRNA) was used to block AGRN gene expression. Finally, enzyme-linked Immunosorbent Assay (ELISA) was used to measure AGRN protein expression in 100 healthy volunteers, 100 CHB patients, and 100 LF/LC patients, and the efficacy of the diagnostic model was assessed by the Area Under the Curve (AUC).

Results. AGRN mRNA displayed a steady rise in the PBMCs of normal, CHB, and LF/LC patients. Besides, AGRN expression was markedly elevated in activated LX2 cells, whereas the expression of COL1 and α-SMA decreased when AGRN was inhibited using siRNA. In addition, downregulation of AGRN can reduce the gene expression of β-catenin and c-MYC while upregulating the expression of GSK-3β. Furthermore, PLT and AGRN were used to develop a non-invasive diagnostic model (PA). To identify CHB patients from healthy subjects, the AUC of the PA model was 0.951, with a sensitivity of 87.0% and a specificity of 91.0%. The AUC of the PA model was 0.922 with a sensitivity of 82.0% and a specificity of 90.0% when differentiating between LF/LC and CHB patients.

Conclusion. The current study indicated that AGRN could be a potential plasma biomarker and the established PA model could improve the diagnostic accuracy for HBV-related liver diseases.

Key words: Biomarker, HBV-associated liver diseases, Chronic hepatitis B, Liver fibrosis/cirrhosis, AGRN

Introduction

Chronic hepatitis B (CHB) is an overlying inflammatory liver disease due to persistent hepatitis B virus (HBV) infection, which is a major public health issue worldwide. Studies have indicated that the persistence or recurrence of inflammatory necrosis gives rise to the development of CHB in individuals with chronic HBV infection. CHB could gradually progress to liver fibrosis, cirrhosis, and even hepatic carcinoma (Lok and Kim, 2007). However, the pathophysiology of chronic HBV infection has not yet been fully understood (Bertoletti and Ferrari, 2012; Cornberg et al., 2017). HBV induces hepatocellular lesions through specific immune reactions and cytokine release, rather than via direct viral damage or insufficient immune response (Shih et al., 2018; Sarmati and Malagnino, 2019). Excessive extracellular matrix (ECM) deposition in response to liver injury leads to liver fibrosis, which serves as a compensatory response to chronic liver damage (Bataller and Brenner., 2005). Recent studies have shown that liver fibrosis and cirrhosis are dynamic and potentially reversible (Masatsugu et al., 2018). Accordingly, the precise diagnosis of liver fibrosis/cirrhosis is essential for improving the prognosis of CHB, preventing complications, and reducing the

Corresponding Author: Yuemin Nan, Department of Traditional and Western Medical Hepatology, Third Hospital of Hebei Medical University, No. 139 Ziqiang Road, 050051 Shijiazhuang, Hebei Province, China. e-mail: nanyuemin@163.com or nanyuemin@hebmu.edu.cn

www.hh.um.es. DOI: 10.14670/HH-18-695

mortality and disease burden associated with HBV infection (Kim et al., 2012; Lo and Kim, 2017).

Presently, the gold standard for diagnosing liver fibrosis/cirrhosis is pathological histological assessment, which, due to its invasive nature, imposes limitations on its clinical application (Kose et al., 2015). In consequence, non-invasive indices such as aminotransferase-to-platelet ratio (APRI) and fibrosis-4 (FIB-4) are commonly used to predict liver fibrosis/cirrhosis in chronic viral hepatitis (Sterling et al., 2006; Xiao et al., 2014). Due to advancements in molecular biology, biomarkers play a crucial role in the early diagnosis and monitoring of various diseases. Some recent clinical studies have focused on identifying valuable biomarkers to assess HBV-related hepatic disorders (Jin et al., 2015; Wu et al., 2015).

Our previous research revealed that transcriptome sequencing (RNA-Seq) analysis of liver tissues from healthy volunteers, CHB patients, and liver fibrosis/cirrhosis (LF/LC) patients identified 348 differentially expressed genes exhibiting a progressively increasing trend across those three cohorts. In this study, we performed GO/KEGG pathway enrichment analysis and identified six genes (*AGRN*, *JAG1*, *CCL5*, *ID3*, *CCND1*, *CAPN2*) closely associated with CHB and LF pathways, which were subsequently investigated as potential biomarkers. By comparing the differential expression of the six genes between LF/LC patients, CHB patients, and healthy controls and exploring the mechanism *in vitro*, AGRN was identified as a new biomarker for predicting the progression of HBV-associated hepatic diseases.

Materials and methods

Study Population

Our study is a single-center cross-sectional study. Blood samples were taken from 100 CHB patients and 100 LF/LC patients who were admitted to the Department of Traditional and Western Medical Hepatology, Third Hospital of Hebei Medical University from January 2020 to December 2021. The control group consisted of 100 healthy individuals who were admitted for physical examinations in the same period. Inclusion criteria were as follows: (1) Adult patients (>18 years); (2) Diagnosed based on widely accepted clinical guidelines for CHB and LF/LC; (3) Child-Pugh score <7 (grade A); (4) Willing to give written informed consent. Exclusion criteria were as follows: (1) Co-infection with human immunodeficiency virus (HIV) or other hepatotropic viruses; (2) Decompensated cirrhosis; (3) Chronic liver disease from other causes; (4) Complicated with severe cardiovascular, pulmonary, or renal diseases, or malignant tumors. Patients' basic clinical information and laboratory results were collected. All procedures were performed after Ethical approval by the Ethics Committee of the Third Hospital of Hebei Medical University. Following centrifugation at 1,000 g for 5 min, the serum was extracted and kept at -80°C. From each group, 20 serum samples were randomly chosen for peripheral blood mononuclear cell (PBMC) extraction. PBMCs were quickly separated and kept at -80°C.

Cell culture

LX2 (human hepatic stellate cell line) was obtained from Shanghai Cell and Molecular Biology Research Center. LX2 cells were cultured in Dulbecco's Modified Eagle Medium (DMEM) medium with 10% Fetal Bovine Serum (FBS) and 1% penicillin/streptomycin solution in an incubator set to 37°C and 5% CO_2.

Cell stimulation by TGF-β1

LX2 cells were cultured in 6-well plates at a density of 3×10^5 cells/well with 2 ml of Complete Growth Medium at the beginning of the process. Serum-free Media was used once cell confluence reached about 60%. After 1h, recombinant human TGF-β1 was added at final concentrations of 2 ng/ml, 5 ng/ml, and 10 ng/ml, respectively. Both TGF-β1 treated cells and untreated control cells were collected after 48h. In addition, cells treated with 10 ng/ml of TGF-β1 were harvested after 12, 24, and 48h.

Cell transfection

LX2 cells were seeded in 6-well plates the day before transfection. When cell confluence reached 30-50%, small-interfering RNAs (siRNAs) were transfected via Lipofectamine™ 2000 (Invitrogen), according to the manufacturer's recommendations. Serum-free media was replaced 6 h after transfection and the cells were cultured in a cell incubator. Three siRNAs were designed against AGRN, and a non-targeting control siRNA (NC-siRNA) was employed as a negative control (all synthesized by Shanghai GenePharma, Co., Ltd). SiRNA sequences are shown in Table 1. Lipofectamine™ 2000 was used as a positive transfection control. A null group was incubated under normal conditions without siRNA transfection. The final concentration of siRNA was 30 nM. TGF-β1 was added 24h later. Transfected cells were harvested 48h later.

RNA extraction and quantitative real-time PCR

Total RNA was extracted from PBMCs of the three groups and LX2 cells using TRIzol (Invitrogen). For reverse transcription, the PrimeScript RT reagent Kit with gDNA Eraser (TaKaRa, Dalian, China) was used according to the instructions of the manufacturer. The reverse transcription procedure was carried out at 37°C for 15 minutes, then at 85°C for 5 seconds; cDNA

samples were kept at -20°C.

The following thermocycling parameters were used in the amplification reactions using TB Green Premix Ex Taq II (TaKaRa, Dalian, China) on the ABI 7500 Real-Time quantitative PCR System: 95°C for 30 sec; followed by 40 cycles of 95°C for 5 sec and 60°C for 34 sec. The primer sequences used are listed in Table 1. Gene expression was compared to *GAPDH* as a reference. The biological and technical duplicates of each sample were repeated three times on a single plate. The $2^{-\Delta\Delta CT}$ approach was utilized to calculate relative gene expression (Livak and Schmittgen, 2001).

Enzyme-linked immunosorbent assay (ELISA)

The levels of plasma AGRN were determined using an ELISA kit from Shanghai Zcibio Biotechnology Co. Ltd. All procedures were performed following the manufacturer's instructions.

Statistical analysis

Baseline characteristics are presented using descriptive statistics with mean or median for continuous variables and numbers or frequencies (%) for categorical variables. Normality and homogeneity of variance for continuous variables were tested using Shapiro-Wilk and Levene's tests, respectively. Differences between groups were assessed using parametric (LSD or t-test) and nonparametric (Kruskal-Wallis or Mann-Whitney U) statistics for continuous variables, and χ^2 tests for categorical variables. Univariate and multivariate logistic regression models were applied. The diagnostic accuracy was evaluated using the Receiver Operating Characteristics Curve (ROC). All statistical analyses were performed using GraphPad Prism 9.0, MedCalc 15.0, and SPSS 26.0. Differences were considered significant when the P value <0.05.

Results

AGRN, JAG1, CCL5, ID3, CCND1, and CAPN2 mRNA expression levels in human PBMCs

The expression of *AGRN*, *JAG1*, *CCL5*, *ID3*, *CCND1*, and *CAPN2* mRNAs in human PBMCs was detected by quantitative real-time PCR (qRT-PCR) (Fig. 1A). Consistent with the results of RNA-Seq, the expression levels of the six genes were all higher in the CHB group than in the control group. Of these, *AGRN*, *JAG1*, *ID3*, and *CAPN2* were significantly upregulated. *JAG1* mRNA levels in the LF/LC group were greater than in CHB but the difference was not statistically significant. However, the expression of *CCL5*, *ID3*, *CCND1*, and *CAPN2* were downregulated in the LF/LC group. Only the expression of *AGRN* significantly increased in all three groups. These findings suggest that AGRN might be implicated and meaningful in CHB and LF/LC development.

Fibrosis-associated gene expression in LX2 cells

According to previous studies, TGF-β1 is the main cytokine involved in hepatic stellate cell (HSC) stimulation and liver fibrosis development (Bi et al., 2012). We stimulated LX2 cells with various TGF-β1 doses and activation durations to determine the best stimulation concentration and time. qRT-PCR was used to evaluate the relative mRNA expression of *COL1* and *α-SMA*. TGF-β1 stimulation increased COL1 and α-SMA expression (Fig. 1B,C) in a time- and dose-dependent manner; *COL1* and *α-SMA* mRNA were higher in the 10 ng/ml TGF-β1 group after 48h. As a result, 10 ng/ml TGF-β1 was used to activate LX2 for 48 hours in the next step.

Table 1. Sequences and oligonucleotides used in our study.

Gene	Forward Sequence (5′ to 3′)	Reverse Sequence (5′ to 3′)
AGRN	GTCCTGCGTCTGCAAGAAGAG	CTCGCATTCGTTGCTGTAGG
JAG1	GTCCATGCAGAACGTGAACG	GCGGGACTGATACTCCTTGA
CCL5	CCAGCAGTCGTCTTTGTCAC	CTCTGGGTTGGCACACACTT
ID3	GAGAGGCACTCAGCTTAGCC	TCCTTTTGTCGTTGGAGATGAC
CCND1	GCTGCGAAGTGGAAACCATC	CCTCCTTCTGCACACATTTGAA
CAPN2	GTTCTGGCAATACGGCGAGT	CTTCGGCTGAATGCACAAAGA
COL1	GAGGGCCAAGACGAAGACATC	CAGATCACGTCATCGCACAAC
α-SMA	AAAAGACAGCTACGTGGGTGA	GCCATGTTCTATCGGGTACTTC
β-catenin	AAAGCGGCTGTTAGTCACTGG	CGAGTCATTGCATACTGTCCAT
GSK-3β	GGCAGCATGAAAGTTAGCAGA	GGCGACCAGTTCTCCTGAATC
c-MYC	GGCTCCTGGCAAAAGGTCA	CTGCGTAGTTGTGCTGATGT
GAPDH	GGAGCGAGATCCCTCCAAAAT	GGCTGTTGTCATACTTCTCATGG
AGRN-siRNA-1	GCACGUAUGACAGUGAUUGTT	CAAUCACUGUCAUACGUGCTT
AGRN-siRNA-2	GCCAGGAGAAUGUCUUCAATT	UUGAAGACAUUCUCCUGGCTT
AGRN-siRNA-3	GCGGUACUUGAAGGGCAAATT	UUUGCCCUUCAAGUACCGCTT
AGRN-siRNA-NC	UUCUCCGAACGUGUCACGUTT	ACGUGACACGUUCGGAGAATT

AGRN, JAG1, CCL5, ID3, CCND1, and CAPN2 mRNA expression levels in LX2 cells

qRT-PCR was used to evaluate the expression of *AGRN*, *JAG1*, *CCL5*, *ID3*, *CCND1*, and *CAPN2* mRNA in LX2 cells. LX2 cells were stimulated with 10 ng/ml TGF-β1 over 48 h, with unstimulated cells serving as the control group. As shown in Fig. 1D, the expression levels of *AGRN*, *JAG1*, and *CCL5* mRNA in the stimulated group were significantly higher than in the unstimulated control group. Up to about a 4-fold increase in AGRN gene expression was observed. However, *ID3*, *CCND1*, and *CAPN2* were down-regulated by 25.1%, 48.9%, and 33.2%, respectively, compared with the control group. *AGRN* mRNA was dramatically elevated in activated LX2 cells and exhibited a progressively increasing trend in PBMCs from normal subjects, CHB, and LF/LC patients. This indicates that AGRN can be a biomarker of CHB and LF/LC. Therefore, we chose the *AGRN* gene for further investigation.

AGRN expression is successfully silenced by siRNAs

With the use of siRNA, genetic knockdown of AGRN was carried out to examine the function of AGRN. As shown in Fig. 2A, 48h after transfection with siRNA, the $2^{-\Delta\Delta Ct}$ values of *AGRN* calculated by the relative quantitative method for the siRNA-1, siRNA-2, and siRNA-3 groups were 0.31±0.03, 0.31±0.07, and 0.54±0.07, respectively. The expression of *AGRN* mRNA measured by qRT-PCR was considerably lower in all three siRNA groups than in the NC group. However, the differences were not statistically significant between the null, Lipo, and NC groups. These findings show that siRNAs effectively suppress *AGRN* mRNA expression. The siRNA silencing efficiency was calculated using the following formula: siRNA silencing efficiency=(1-AGRN expression in the siRNA group/AGRN expression in the blank group) × 100%. SiRNA-1 and siRNA-2 exhibited the highest inhibition efficacy, therefore, these were used in subsequent experiments. LX2 cells were transfected with

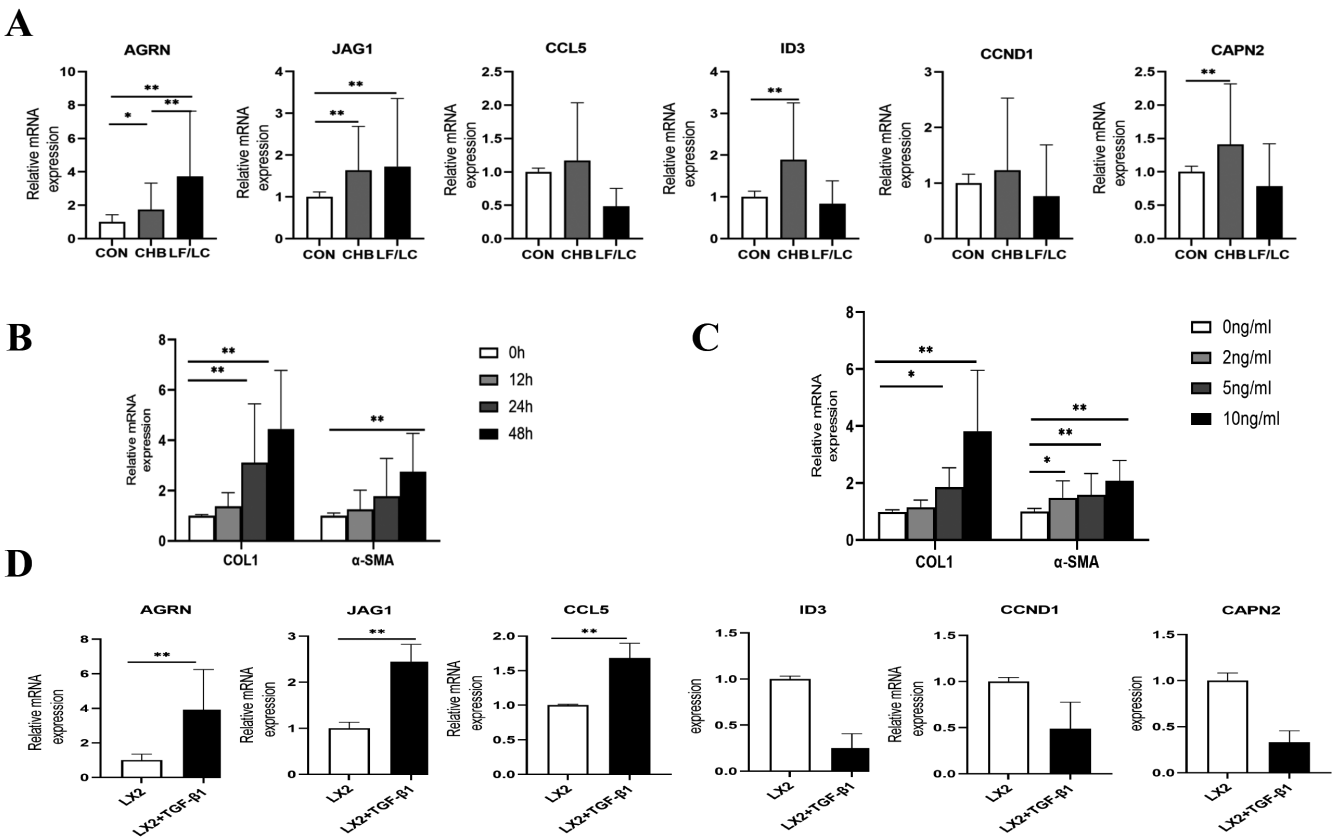

Fig. 1. A. qRT-PCR validation of differentially expressed genes in the transcriptome sequencing of human PBMCs (n=20). Data are shown as mean ± SD. The results were normalized based on the housekeeping gene *GAPDH*. The expression of *COL1* and *α-SMA* mRNA in LX2 cells stimulated by TGF-β1 at different time intervals and concentrations using qRT-PCR. **B.** LX2 cells were stimulated with TGF-β1 (10 ng/ml) for 0, 12, 24, and 48h, respectively. **C.** LX2 cells were stimulated with TGF-β1 (0 ng/ml, 2 ng/ml, 5 ng/ml, and 10 ng/ml) for 48h. Data are shown as mean ± SD. The results were normalized based on the housekeeping gene *GAPDH*. **D.** qRT-PCR validation of differentially expressed genes in the transcriptome sequencing in LX2 cells. Cells were stimulated with TGF-β1 (10 ng/ml) for 48h. Cells were stimulated without TGF-β1 as control. Data are shown as the mean ± SD. The results were normalized based on the housekeeping genes GAPDH. **P*<0.05, ***P*<0.01.

an AGRN-targeting siRNA and a negative control siRNA. Then, cells were stimulated with 10 ng/ml TGF-β1 for 24h. As seen in Figure 2B-D, TGF-β1 dramatically enhanced the expression of *AGRN*, *COL1*, and α-SMA compared with the control group, whether or not a negative control siRNA was transfected. After AGRN inhibition by siRNA, the expression of COL1 and *α-SMA* was markedly reduced in active LX2 cells. Thus, AGRN may play a pivotal role in regulating the synthesis and secretion of *COL1* and α-SMA in activated LX2 cells and liver fibrosis.

SiRNA-AGRN suppresses Wnt/β-catenin signaling

Agrin, a heparan sulfate proteoglycan, is a crucial component of the basal lamina facilitating acetylcholine receptor clustering for proper neuromuscular junction (NMJ) function (Bolliger et al., 2010). It has been demonstrated that AGRN can stimulate the classical Wnt/β-catenin signaling pathway to mediate the biological role of NMJ formation (Ohno et al., 2017). The Wnt/β-catenin signaling pathway contributes to liver fibrosis (Miao et al., 2013). β-catenin, a transcription factor, acts as the main effector of the canonical Wnt signaling pathway. Accumulation of β-catenin in the nucleus activates the canonical Wnt/β-catenin pathway (Schmalhofer et al., 2009). According to our qRT-PCR results (Fig. 2E-G), AGRN inhibition in LX2 cells reduced the expression of β-catenin and downstream c-MYC; concurrently, GSK-3β expression was elevated. GSK-3β, β-catenin, and c-MYC are major signaling proteins in the Wnt/β-catenin signaling pathway. As a result, we anticipated that decreasing AGRN expression would result in decreased ECM expression in activated LX2 cells by blocking the Wnt/β-catenin signaling pathway.

The protein levels of AGRN via ELISA and demographic and clinical characteristics

ELISA was performed to measure protein levels. Our study showed that, compared with the control group, the protein levels of AGRN were significantly increased in the CHB and LF/LC groups. Furthermore, the AGRN protein level was markedly higher in the LF/LC than in the CHB group (Table 2). The demographic and clinical characteristics of patients and healthy subjects are also shown in Table 2. As demonstrated in Table 2, male patients are more common in CHB and LF/LC, particularly LF/LC. Furthermore, age, aspartate aminotransferase (AST), and total bilirubin (TBIL) levels gradually increased across the three groups. However, the expression of white blood cells (WBC), platelet count (PLT), total protein (TP), and albumin (ALB) significantly decreased with disease progression. The differences were statistically significant.

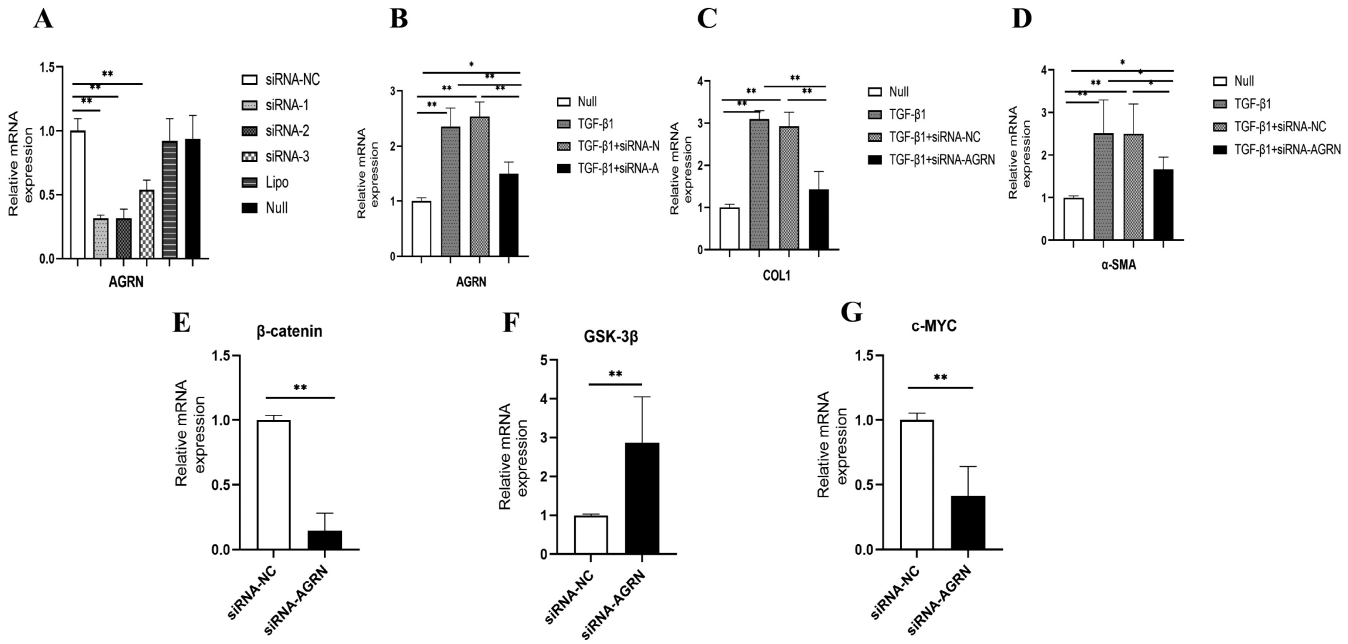

Fig. 2. Effect of gene-specific AGRN siRNA on the fibrotic markers of LX2 cells. **A.** Comparison of *AGRN* mRNA expression levels among siRNA, Lipo, and Null groups after transfection with three siRNA-AGRN oligonucleotide sequences and siRNA-NC. **B.** qRT-PCR detected the expression of AGRN of each experimental group at 24h after 10 ng/ml TGF-β1 treatment. **C, D.** The effect of siRNA-AGRN knockdown on the expression of the fibrotic markers COL1 **(C)** and α-SMA **(D)** was determined using qRT-PCR at 24h after 10 ng/ml TGF-β1 treatment. **E-G.** Effect of silencing AGRN by siRNA on major genes of the canonical Wnt/β-catenin signaling pathway in LX2 cells. Data are shown as mean ± SD. qRT-PCR results were normalized to the housekeeping gene *GAPDH*. **P*<0.05, ***P*<0.01.

Univariate and multivariate ordinal logistic regression analyses

In order to find important covariates, a univariate regression analysis was performed. Table 3 shows that eight variables, including gender (man), age, WBC, PLT, ALB, AST, TBIL, and AGRN were significantly associated with the incidence of CHB and LF/LC. As TP was not significantly related, it was not included in subsequent analyses. The components showing significant differences in the univariate logistic regression were used in the multivariate logistic regression study. The results showed that PLT (OR = 0.992; 95% CI= 0.989-0.995; $P<0.001$) and AGRN (OR =3.010; 95% CI=2.455-3.691; $P<0.001$) were significantly and independently associated with CHB and LF/LC. We developed a regression equation integrating relevant markers to differentiate between healthy subjects, CHB patients, and LF/LC patients: PA = 1.639 - 0.008×PLT + 1.102×AGRN.

Predictive value of the regression model

ROC analysis was used to assess the predictive value of PA in differentiating between healthy, CHB, and LF/LC. As shown in Table 4 and Figure 3, the PA model's area under the curve (AUC) for predicting CHB was 0.951, which was greater than the APRI and FIB-4 models. It had a sensitivity of 87.0% and a specificity of 91.0%. The optimum cut-off value for distinguishing

Table 2. Clinical and laboratory characteristics of the participants.

Variables	CONTROL (N=100)	CHB (N=100)	LF/LC (N=100)	F/Z/X2	*P*
Gender (male), n (%)	45 (45.0)	65 (65.0) *	73 (73.0) *	17.486	0.000
Age (years)	33.0 (27.0-41.0)	42.0 (34.0-52.0) *	49.0 (38.5-58.0) *#	54.478	0.000
WBC (10^9/L)	5.9 (5.1-7.4)	4.9 (4.1-6.0) *	4.6 (3.1-5.8) *	44.493	0.000
RBC (10^{12}/L)	4.6 (4.5-5.0)	4.7 (4.3-5.1)	4.5 (3.9-4.8) *#	11.360	0.003
HGB (g/L)	140.9 (133.2-153.9)	144.0 (130.0-155.0)	137.0 (120.5-151.0) *	6.593	0.037
MCV (fL)	—	91.9 (88.7-94.6)	90.9 (86.0-93.2) #	-1.851	0.064
PLT (10^9/L)	232.8 (201.6-264.9)	200.6 (148.0-241.0) *	125.0 (75.5-169.5) *#	93.711	0.000
TP (g/L)	73.6 (71.8-76.5)	72.3 (64.8-75.4) *	68.8 (63.9-74.5) *	37.103	0.000
ALB (g/L)	45.8 (43.2-48.2)	45.0 (38.6-47.9) *	41.1 (36.1-45.0) *#	41.006	0.000
ALT (U/L)	17.0 (13.0-24.3)	39.0 (20.0-118.0) *	37.0 (21.0-157.0) *	69.424	0.000
AST (U/L)	17.5 (15.0-21.0)	27.0 (20.0-70.0) *	38.0 (22.0-98.0) *	88.140	0.000
TBIL (μmol/L)	16.2 (12.6-18.9)	17.0 (13.4-24.5) *	19.4 (14.5-32.5) *	17.503	0.000
DBIL (μmol/L)	—	8.3 (5.0-10.9)	7.8 (4.1-13.2) #	-2.876	0.004
ALP (U/L)	—	85.0 (66.0-103.0)	76.5 (63.0-109.8) #	-2.643	0.008
GGT (U/L)	—	60.0 (26.0-136.0)	47.0 (24.5-104.8) #	-2.712	0.007
CHE (U/L)	—	8.4±3.0	5.7±2.6 #	-5.912	0.000
TBA (μmol/L)	—	8.2 (3.4-20.1)	9.5 (4.3-28.5) #	-3.801	0.000
CK (U/L)	—	62.7 (45.1-90.6)	77.0 (56.4-114.9)	-1.360	0.174
LDH (U/L)	—	193.1±85.7	212.4±127.7	-1.708	0.088
TCHO (mmol/L)	—	4.1 (3.6-4.7)	4.0 (3.4-4.3) #	-3.656	0.000
TG (mmol/L)	—	1.2 (0.7-1.7)	1.1 (0.7-1.3) #	-1.980	0.048
GLU (mmol/L)	5.0 (4.5-5.5)	5.4 (4.9-5.9) *	5.2 (4.7-5.7) *	13.890	0.001
Urea (mmol/L)	4.6 (3.6-5.4)	4.4 (3.7-5.4)	4.7 (3.7-5.6)	1.151	0.563
CREA (μmol/L)	64.3 (55.6-77.3)	66.3 (55.0-77.4)	61.4 (51.5-68.8) *#	8.282	0.016
URIC (μmol/L)	289.0 (239.5-353.5)	322.0 (261.0-389.0)	283.0 (216.0-337.0) #	9.046	0.011
Ca (mmol/L)	—	2.4±0.1	2.3±0.2 #	3.044	0.000
PHOS (mmol/L)	—	1.1±0.2	1.1±0.2	0.420	0.357
CRP (mg/L)	—	2.2 (1.6-3.2)	1.9 (1.6-3.4)	-0.557	0.577
PT (s)	—	12.0 (11.0-13.0)	12.0 (11.2-13.5)	-1.804	0.071
INR	—	1.1 (1.0-1.2)	1.0 (1.0-1.2) #	-2.832	0.005
HBsAg ($\log_{10}$ IU/mL)	—	3.1 (2.4-4.0)	2.8 (2.3-3.2) #	-3.245	0.001
HBVDNA ($\log_{10}$ IU/mL)	—	2.7 (1.3-6.0)	2.3 (1.3-5.0)	-0.061	0.289
AFP (ng/mL)	—	3.8 (2.6-13.7)	4.5 (2.2-26.9) #	-2.513	0.012
Ferritin (ng/mL)	—	128.4 (39.0-365.4)	157.2 (65.7-267.6) #	-1.917	0.055
LSM (kPa)	—	7.6 (5.3-10.9)	13.7 (10.3-19.3) #	6.001	0.000
FIB-4	0.5 (0.4-0.6)	1.1 (0.7-2.1) *	2.9 (1.5-5.5) *#	234.977	0.000
APRI	0.2 (0.1-0.3)	0.4 (0.2-1.1) *	1.1 (0.5-2.4) *#	216.240	0.000
AGRN (ng/mL)	2.8 (2.1-3.5)	4.8 (4.0-5.5) *	6.3 (5.5-7.4) *#	219.056	0.000

*$P<0.05$ vs. healthy control; #$P<0.05$ vs. chronic hepatitis B. WBC, white blood cell; RBC, red blood cell; HGB, hemoglobin; MCV, mean corpuscular volume; PLT, platelet; TP, total protein; ALB, albumin; ALT, alanine aminotransferase; AST, aspartate aminotransferase; TBIL, total bilirubin; DBIL, direct bilirubin; ALP, alkaline phosphatase; GGT, gamma-glutamyl transferase; CHE, cholinesterase; TBA, total bile acid; CK, creatine kinase; LDH, lactate dehydrogenase; TCHO, total cholesterol; TG, triglyceride; GLU, glucose; CREA, creatinine; Ca, calcium; PHOS, phosphorus; CRP, C-reactive protein; PT, prothrombin time; INR, international normalized ratio; HBsAg, hepatitis B surface antigen; HBVDNA, hepatitis B virus deoxyribonucleic acid; AFP, alpha fetoprotein; LSM, liver stiffness measurement; FIB-4, fibrosis index based on the 4 factors; APRI, AST-to-PLT ratio index; AGRN, agrin; CHB, chronic hepatitis B; LF/LC, liver fibrosis/liver cirrhosis.

CHB patients from healthy subjects was 4.278. In addition, PA was superior to APRI, FIB-4, and even Liver stiffness measurement (LSM) in predicting liver cirrhosis, with AUC values of 0.922, 0.663, 0.725, and 0.768, respectively. The cut-off value was 6.645, with 82.0% sensitivity and 90.0% specificity. Overall, our study found that a unique PA model may be used to distinguish CHB from healthy individuals and LF/LC from CHB. This model is non-invasive, easy to use, and cost-effective.

Discussion

CHB is a global health issue, which affects approximately 257 million people worldwide (Nguyen et al., 2020). In China, it is estimated that there are around

Table 3. Univariate and multivariate ordinal logistic analyses for the variables.

Variables	Univariate ordinal logistic analyses		Multivariate ordinal logistic analyses	
	OR (95% CI)	*P*	OR (95% CI)	*P*
Gender (male), n (%)	0.402 (0.259-0.624)	<0.001		
Age (years)	1.069 (1.050-1.090)	<0.001		
WBC (10^9/L)	0.797 (0.733-0.866)	<0.001		
PLT (10^9/L)	0.984 (0.981-0.988)	<0.001	0.992 (0.989-0.995)	<0.001
TP (g/L)	1.000 (0.999-1.002)	0.422		
ALB (g/L)	0.882 (0.849-0.918)	<0.001		
AST (U/L)	1.006 (1.003-1.010)	<0.001		
TBIL (μmol/L)	1.017 (1.008-1.025)	<0.001		
AGRN (ng/mL)	9.161 (6.246-13.437)	<0.001	3.010 (2.455-3.691)	<0.001

WBC, white blood cell; PLT, platelet; TP, total protein; ALB, albumin; AST, aspartate aminotransferase; TBIL, total bilirubin; AGRN, agrin.

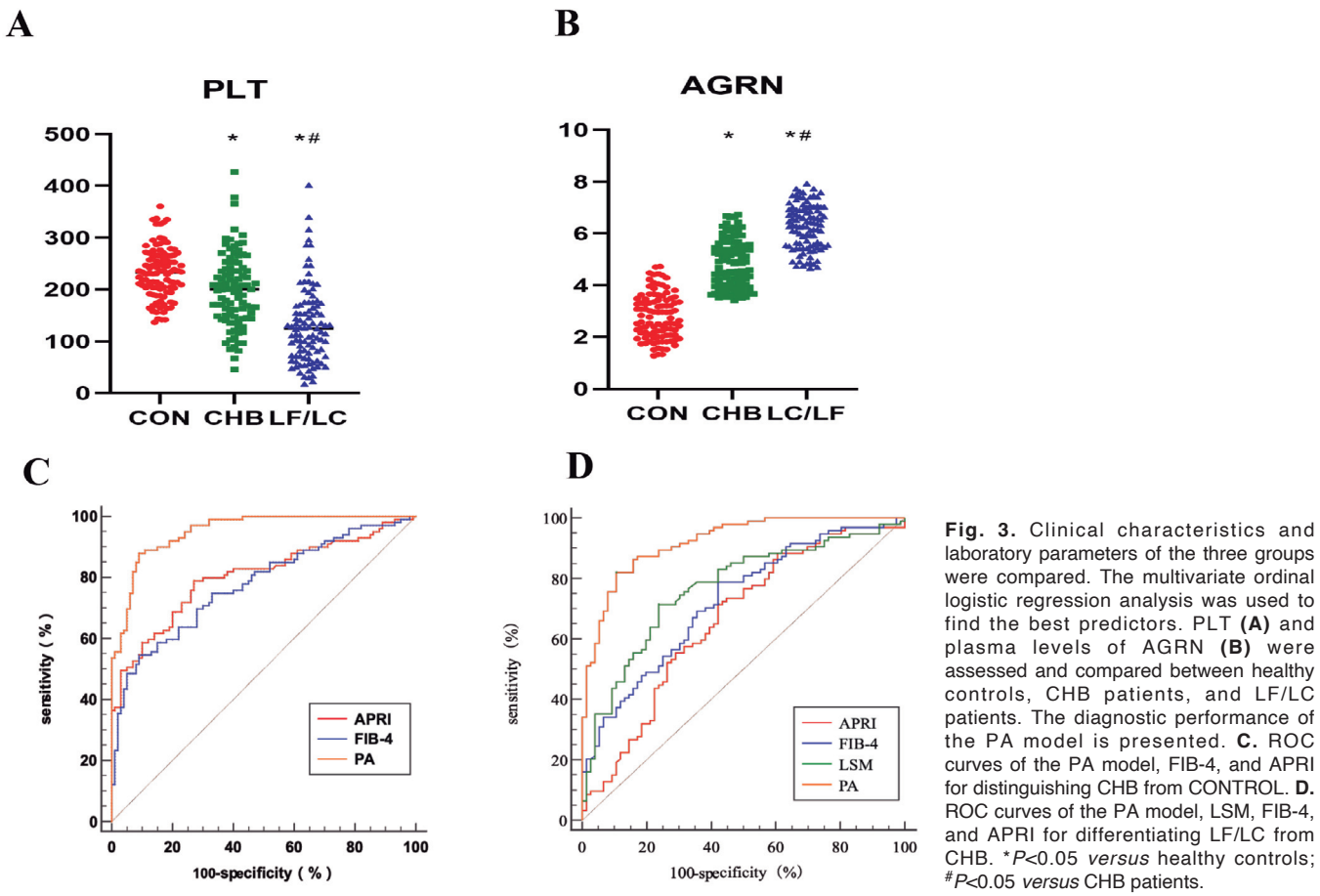

Fig. 3. Clinical characteristics and laboratory parameters of the three groups were compared. The multivariate ordinal logistic regression analysis was used to find the best predictors. PLT **(A)** and plasma levels of AGRN **(B)** were assessed and compared between healthy controls, CHB patients, and LF/LC patients. The diagnostic performance of the PA model is presented. **C.** ROC curves of the PA model, FIB-4, and APRI for distinguishing CHB from CONTROL. **D.** ROC curves of the PA model, LSM, FIB-4, and APRI for differentiating LF/LC from CHB. **P*<0.05 *versus* healthy controls; $^{\#}$*P*<0.05 *versus* CHB patients.

70 million HBV carriers (5-6% prevalence) (Liu et al., 2016), 20 to 30 million people with CHB, 1 million with liver cirrhosis, and 0.3 million with hepatocellular carcinoma caused by HBV (Shan and Jia, 2017). HSC proliferation is associated with the production of collagen and other ECM components. Local collagen deposition leads to advanced liver fibrosis, pseudolobule formation, and eventually cirrhosis. The continuous inflammatory microenvironment, which accelerates the repair and proliferation of hepatocytes, can promote the occurrence of tumors (Llovet et al., 2016; D'Amico et al., 2018).

Given the serious public health concern of complications related to hepatitis B, accurate diagnosis of HBV-associated liver disease is critical. Although liver biopsy remains the gold standard for diagnosing CHB and LF/LC, there are still major concerns, such as sampling error, high bleeding risk, heavy medical burden, interobserver discrepancy, and inability to be repeated, limiting its widespread use in clinical practice (Lok and McMahon, 2009; Venkatesh et al., 2013). Biological markers, such as proteins and DNA, discovered in tissues and bodily fluids (e.g., blood and urine), typically serve as indicators of therapeutic response and disease severity (Birkó et al., 2020). Recently, the non-invasive assessment of HBV-associated liver disease has grown rapidly owing to the stability, wide distribution, and ease of detection of serum biomarkers.

Previous transcriptome sequencing and bio-informatics results from our research group indicated that the *AGRN*, *JAG1*, *CCL5*, *ID3*, *CCND1*, and *CAPN2* genes were differentially expressed in CHB and LF/LC patients compared with healthy controls, and gradually increased with disease progression. In the current investigation, we initially confirmed the expression trend of six genes in PBMCs from healthy participants, CHB patients, and LF/LC patients. We discovered that only *AGRN* gene expression steadily and significantly increased in all three groups. Cell models of HBV infection and replication *in vitro* are important tools for studying HBV-related liver diseases. However, there are many limitations of *in vitro* HBV models established by laboratories at home and abroad, such as low actual infection efficiency, low level of virological indicators after replication, long culture and differentiation cycle, and high infective dose, which greatly limit the application of HBV-related cell models. LX-2 used in this study are immortalized cell lines. Under the stimulation of various factors, HSCs are transformed from the static cell to the myofibroblast phenotype with proliferation, fibroblast, and contraction, which is the activated HSCs (Geerts, 2001). TGF-β has the most significant effect on activating HSC-inducing factors (Kaimori et al., 2007; Nguyen et al., 2007; Zhang et al., 2014; Khanizadeh et al., 2015). Meanwhile, the expression of *AGRN* mRNA was also significantly increased in TGF-β1-activated LX2 cells. In addition, ELISA was used to detect AGRN protein in the three groups, which also showed a progressively increasing trend. These findings imply that AGRN may have a role in the progression of CHB and LF/LC after HBV infection.

AGRN, a heparan sulfate proteoglycan (HSPG), is a component of the ECM (Neill et al., 2015), which plays an important role in skeletal muscle development, NMJ formation, hematopoiesis, and inflammation (Bruno et al., 1995; Jurdana et al., 2009; Zong and Jin., 2013). It is expressed in the hepatic bile duct and vascular basement membrane of the normal liver (Tátrai et al., 2009), which is a specific and sensitive biomarker of hepatocellular carcinoma due to its expression in the microvasculature; however, it has rarely been studied in CHB and LF/LC (Tátrai et al., 2009). Currently known Agrin receptors include MuSK-Lrp4, integrin, dystroglycan 1, and α3 sodium and potassium pump (Zhang et al., 2008). When Agrin interacts with MuSK-Lrp4, it can activate the classical Wnt/β-catenin pathway (Barik et al., 2014). Multiple studies have reported that the abnormal expression of the Wnt/β-catenin signaling pathway is involved in multiple processes of liver disease pathophysiology, such as hepatocyte proliferation, HSC activation, liver fibrosis, cirrhosis, focal nodular hyperplasia, and even the occurrence and development of liver tumors (Perugorria et al., 2019; Rao et al., 2019; Rong et al, 2019; Zhang et al., 2020).

Our results showed that AGRN inhibition by siRNA in activated LX2 cells significantly decreases *COL1* and

Table 4. Comparison of the diagnostic performance of FIB-4, APRI, LSM, and PA in patients with CHB and LF/LC.

	Variables	AUC	Cut-off	Sensitivity	Specificity	Youden index	*P*
CHB	FIB-4	0.775	0.989	54.5	91.0	0.456	<0.0001
	APRI	0.803	0.232	78.0	73.0	0.510	<0.0001
	PA[¶,$]	0.951	4.278	87.0	91.0	0.780	—
LF/LC	LSM	0.768	10.93	71.3	76.3	0.476	0.0002
	FIB-4	0.725	1.446	80.0	63.6	0.436	0.0001
	APRI	0.663	0.479	75.0	61.0	0.360	0.0001
	PA[÷,¶,$]	0.922	6.645	82.0	90.0	0.720	—

[÷]*P*<0.05 vs LSM in AUC; [¶]*P*<0.05 vs FIB-4 in AUC; [$]*P*<0.05 vs. APRI in AUC. LSM, liver stiffness measurement; FIB-4, fibrosis index based on the 4 factors; APRI, AST-to-PLT ratio index; PA, the model based on PLT and AGRN; CHB, chronic hepatitis B; LF/LC, liver fibrosis/liver cirrhosis.

α-SMA expression. Further experiments indicated a significant downregulation of the *β-catenin* gene and its downstream gene *c-MYC*, with a notable upregulation of *GSK-3β* expression after AGRN inhibition. β-catenin, a cytoskeletal protein, serves as a crucial signaling molecule in the regulation of the classical Wnt/β-catenin pathway. When this pathway is inactivated, β-catenin is typically phosphorylated and degraded by the GSK-3β complex. GSK-3β functions as an essential negative regulator and its downregulation reflects the activation of the Wnt/β-catenin signaling pathway (Wu and Pan, 2010). The Wnt/β-catenin pathway promotes the transcription of c-*MYC* (Shi et al., 2007), and is closely linked to liver fibrosis, suggesting that silencing AGRN via siRNA may reduce the development of liver fibrosis by inhibiting the Wnt/β-catenin signaling pathway. Therefore, AGRN can serve as a new therapeutic target for the prevention and treatment of liver fibrosis and may offer fresh perspectives on its clinical management.

Over the past decade, a number of non-invasive techniques, including APRI and FIB-4, have been used to predict liver fibrosis (Xiao et al., 2015). FibroScan is a practical and repeatable non-invasive detection method that is frequently used to identify liver fibrosis (Huang et al., 2021). The ideal non-invasive technique should be straightforward, affordable, trustworthy, and accurate. In this study, a novel model called PA was developed based on PLT and AGRN. Compared to APRI, FIB-4, and LSM, PA had the highest AUC of HBV-related liver diseases and the highest sensitivity and specificity. In the diagnosis of LF/LC, the sensitivity and specificity of the PA model are greater than those of LSM, indicating that the model has a superior diagnostic yield. The PA model can serve as a new reference index for evaluating CHB and LF/LC since it is non-invasive, accurate, and reproducible.

However, there were certain restrictions in our study. First, the sample size of the study was relatively small, and the data included in the present study were from a single center. An optimized cooperative multicenter study is required to verify the model. Furthermore, patients with CHB and LF/LC were not divided based on the use of antiviral drugs. Aside from that, more functional studies are needed to elucidate the function of AGRN in chronic liver disease *in vitro* and *in vivo*.

In conclusion, the current study demonstrated that AGRN might be a potential plasma biomarker for the diagnosis of CHB, and the PA model established achieved higher accuracy and better performance than APRI and FIB-4 in differentiating HBV-related chronic hepatitis and liver fibrosis/cirrhosis.

Funding. This project was supported by the Key Research and Development Program of Hebei Province in 2019 (No. 19277779D); the introduction of foreign intelligence program in Hebei Province in 2020; and the project of provincial subsidy Fund (Construction of key traditional Chinese medicine Disciplines) for inheritance and development of traditional Chinese medicine in 2022.

Competing interests. We declare that we have no financial or personal relationships with other people or organizations that can inappropriately influence our work.

Ethics approval and informed consent. Each participant provided written informed permission, which was also authorized by the Third Hospital of Hebei Medical University's local ethics council.

Data availability. The authors affirm that all pertinent information supporting the conclusions drawn from this investigation is contained in the article and its Supplementary Information files, and, upon reasonable request, is available directly from the corresponding author.

Authors' contributions. Design and writing the article: Rong Ai; cell experiment: Lu Li, Xiwei Yuan; data collection: Chen Dong, Yao Dou, Mengmeng Hou; statistical analysis: Dandan Zhao, Shiming Dong; literature review and evaluation: Tongguo Miao, Weiwei Guan; critical revision of the manuscript and financial support: Yuemin Nan. All authors approved the final version of the manuscript.

References

Barik A., Zhang B., Sohal GS., Xiong W.C. and Mei L. (2014). Crosstalk between Agrin and Wnt signaling pathways in development of vertebrate neuromuscular junction. Dev. Neurobiol. 74, 828-838.

Bataller R. and Brenner D. (2005). Liver fibrosis. J. Clin. Invest. 115, 209-218.

Bertoletti A. and Ferrari C. (2012). Innate and adaptive immune responses in chronic hepatitis B virus infections: towards restoration of immune control of viral infection. Gut 61, 1754-1764.

Bi W.R., Yang C.Q. and Shi Q. (2012). Transforming growth factor-β1 induced epithelial-mesenchymal transition in hepatic fibrosis. Hepatogastroenterology 59, 1960-1963.

Birkó Z., Nagy B., Klekner Á. and Virga J. (2020). Novel molecular markers in glioblastoma-benefits of liquid biopsy. Int. J. Mol. Sci. 21, 7522.

Bolliger M.F., Zurlinden A., Lüscher D., Bütikofer L., Shakhova O. and Francolini M. (2010). Specific proteolytic cleavage of agrin regulates maturation of the neuromuscular junction. J. Cell Sci. 15, 3944-3955.

Bruno E., Luikart S.D., Long M.W. and Hoffman R. (1995). Marrow-derived heparan sulfate proteoglycan mediates the adhesion of hematopoietic progenitor cells to cytokines. Exp. Hematol. 23, 1212-1217.

Cornberg M., Wong V., Locarnini S., Brunetto M., Janssen H. and Chan H. (2017). The role of quantitative hepatitis B surface antigen revisited. J. Hepatol. 66, 398-411.

D'Amico G., Morabito A., D'Amico M., Pasta L., Malizia G. and Rebora P. (2018). New concepts on the clinical course and stratification of compensated and decompensated cirrhosis. Hepatol. Int. 12, 34-43.

European Association for Study of Liver, & Asociacion Latinoamericana para el Estudio del Higado (2015). EASL-ALEH Clinical Practice Guidelines: Non-invasive tests for evaluation of liver disease severity and prognosis. J. Hepatol. 63, 237-264.

Geerts A. (2001). History, heterogeneity, developmental biology, and functions of quiescent hepatic stellate cells. Semin. Liver Dis. 21, 311-336.

Huang L.L., Yu X.P., Li J.L., Lin H.M., Kang N.L. and Jiang.J.J. (2021). Effect of liver inflammation on accuracy of FibroScan device in assessing liver fibrosis stage in patients with chronic hepatitis B virus infection. World J. Gastroenterol. 27, 641-653.

Jin B.X., Zhang Y.H., Jin W.J., Sun X.Y., Qiao G.F. and Wei Y.Y. (2015). MicroRNA panels as disease biomarkers distinguishing hepatitis B virus infection caused hepatitis and liver cirrhosis. Sci. Rep. 12, 15026.

Jurdana M., Fumagalli G., Grubic Z., Lorenzon P., Mars T. and Sciancalepore M. (2009). Neural agrin changes the electrical properties of developing human skeletal muscle cells. Cell. Mol. Neurobiol. 29, 123-131.

Kaimori A., Potter J., Kaimori J.Y., Wang C., Mezey E. and Koteish A. (2007). Transforming growth factor-beta1 induces an epithelial-to-mesenchymal transition state in mouse hepatocytes *in vitro*. J. Biol. Chem. 282, 22089-22101.

Khanizadeh S., Ravanshad M., Hosseini S.Y., Davoodian P., Zadeh A.N. and Sarvari J. (2015). Blocking of smad4 expression by shrna effectively inhibits fibrogenesis of human hepatic stellate cells. Gastroenterol. Hepatol. Bed Bench 8, 262-269.

Kim S.U., Oh H.J., Wanless I.R., Lee S., Han K.H. and Park Y.N. (2012). The Laennec staging system for histological sub-classification of cirrhosis is useful for stratification of prognosis in patients with liver cirrhosis. J. Hepatol. 57, 556-563.

Kose S., Ersan G., Tatar B., Adar P. and Sengel B.E. (2015). Evaluation of percutaneous liver biopsy complications in patients with chronic viral hepatitis. Eurasian J. Med. 47, 161-164.

Liu J., Zhang S.K., Wang Q.M., Shen H.P., Zhang M. and Zhang Y.P. (2016). Seroepidemiology of hepatitis B virus infection in 2 million men aged 21-49 years in rural China: a population-based, cross-sectional study. Lancet Infect. Dis. 16, 80-86.

Livak K.J. and Schmittgen T.D. (2001). Analysis of relative gene expression data using real-time quantitative PCR and the 2(-Delta Delta C(T)) Method. Methods 25, 402-408.

Llovet J.M., Zucman-Rossi J., Pikarsky E., Sangro B., Schwartz M. and Sherman M. (2016). Hepatocellular carcinoma. Nat. Rev. Dis. Primers 2, 16018.

Lo R.C. and Kim H. (2017). Histopathological evaluation of liver fibrosis and cirrhosis regression. Clin. Mol. Hepatol. 23, 302-307.

Lok A.S. and McMahon B.J. (2007). Chronic hepatitis B. Hepatology 45, 507-539.

Lok A.S. and McMahon B.J. (2009). Chronic hepatitis B: update 2009. Hepatology 50, 661-662.

Masatsugu O., Shunsuke O., Hidetaka H., Koji Y., Qingjie F. and Osamu M. (2018). Palmitoylethanolamide ameliorates carbon tetrachloride-induced liver fibrosis in rats. Front. Pharmacol. 9, 709.

Miao C.G., Yang Y.Y., He X., Huang C., Huang Y. and Zhang L. (2013). Wnt signaling in liver fibrosis: Progress, challenges and potential directions. Biochimie 95, 2326-2335.

Neill T., Schaefer L. and Iozzo R.V. (2015). Decoding the matrix: instructive roles of proteoglycan receptors. Biochemistry 54, 4583-98.

Nguyen L.N., Furuya M.H., Wolfraim L.A., Nguyen A.P., Holdren M.S., Campbell J.S., Knight B., Yeoh G.C., Fausto N. and Parks W.T. (2007). Transforming growth factor-beta differentially regulates oval cell and hepatocyte proliferation. Hepatology 45, 31-41.

Nguyen M.H., Wong G., Gane E., Kao J.H. and Dusheiko G. (2020). Hepatitis B Virus: Advances in Prevention, Diagnosis, and Therapy. Clin. Microbiol. 33, e00046-19.

Ohno K., Rahman M.A., Nazim M., Nasrin F., Lin Y. and Takeda J.I. (2017). Splicing regulation and dysregulation of cholinergic genes expressed at the neuromuscular junction. J. Neurochem. 142, 64-72.

Perugorria M.J., Olaizola P., Labiano I., Esparza-Baquer A., Marzioni M., Marin J.J.G., Bujanda L. and Banales J.M. (2019). Wnt-β-catenin signalling in liver development, health and disease. Nat. Rev. Gastroenterol. Hepatol. 16, 121-136.

Rao S., Xiang J., Huang J., Zhang S., Zhang M., Sun H. and Li J. (2019). PRC1 promotes GLI1-dependent osteopontin expression in association with the Wnt/β-catenin signaling pathway and aggravates liver fibrosis. Cell Biosci. 9, 100.

Rong X., Liu J., Yao X., Jiang T., Wang Y. and Xie F. (2019). Human bone marrow mesenchymal stem cells-derived exosomes alleviate liver fibrosis through the Wnt/β-catenin pathway. Stem. Cell Res. Ther. 10, 98.

Sarmati L. and Malagnino V. (2019). HBV Infection in HIV-Driven Immune Suppression. Viruses 11, 1077.

Schmalhofer O., Brabletz S. and Brabletz T. (2009). E-cadherin, β-catenin, and ZEB1 in malignant progression of cancer. Cancer Metastasis Rev. 28, 151-166.

Shan S. and Jia J.D. (2017). Advances and challenge in prevention and treatment of hepatitis B in China. Chin. J. Viral Dis. 7, 5-8.

Shi B., Liang J., Yang X, Wang Y., Zhao Y. and Wu H. (2007). Integration of Estrogen and Wnt Signaling Circuits by the Polycomb Group Protein EZH2 in Breast Cancer Cells. Mol. Cell. Biol. 27, 5105-5119.

Shih C., Yang C.C., Choijilsuren G., Chang C.H. and Liou A.T. (2018). Hepatitis B Virus. Trends Microbiol. 26, 386-387.

Sterling R.K., Lissen E. and Clumeck N. (2006). Development of a simple noninvasive index to predict significant fibrosis in patients with HIV/HCV coinfection. Hepatology 43, 1317-1325.

Tátrai P., Somorácz A., Batmunkh E., Schirmacher P. and Kovalszky I. (2009). Agrin and CD34 Immunohistochemistry for the Discrimination of Benign *Versus* Malignant Hepatocellular Lesions. Am. J. Surg. Pathol. 33, 874-885.

Venkatesh S.K., Yin M. and Ehman R.L. (2013). Magnetic resonance elastography of liver: technique, analysis, and clinical applications. J. Magn. Reson. Imaging 37, 544-555.

Wu D. and Pan W. (2010). GSK3: a multifaceted kinase in Wnt signaling. Trends Biochem. Sci. 35, 161-168.

Wu C., Liu L., Zhao P., Tang D. and Wang Z.Q. (2015). Potential serum markers for monitoring the progression of hepatitis B virus-associated chronic hepatic lesions to liver cirrhosis. Gut Liver 9, 665-671.

Xiao G., Yang J. and Yan L. (2014). Comparison of Diagnostic accuracy of APRI and FIB-4 for detecting liver fibrosis in adult patients with chronic hepatitis B virus infection: A systemic review and meta-analysis. Hepatology 61, 292-302.

Xiao G., Yang J. and Yan L. (2015). Comparison of diagnostic accuracy of aspartate aminotransferase to platelet ratio index and fibrosis-4 index for detecting liver fibrosis in adult patients with chronic hepatitis B virus infection: a systemic review and meta-analysis. Hepatology 61, 292-302.

Zhang B., Luo S., Wang Q., Suzuki T., Xiong W.C. and Mei L. (2008). LRP4 serves as a coreceptor of agrin. Neuron 60, 285-297.

Zhang M., Haughey M., Wang N.Y., Blease K., Kapoun A.M., Couto S., Belka I., Hoey T., Groza M., Hartke J., Bennett B., Cain J., Gurney A., Benish B., Castiglioni P., Drew C., Lachowicz J., Carayannopoulos L., Nathan S.D., Distler J., Brenner D.A., Hariharan K., Cho H. and Xie W. (2020). Targeting the Wnt signaling pathway through R-spondin 3 identifies an anti-fibrosis treatment strategy for multiple organs. PLoS One 15, e0229445.

Zhang S., Sun W.Y., Wu J.J. and Wei W. (2014). TGF-β signaling pathway as a pharmacological target in liver diseases. Pharmacol. Res. 85, 15-22.

Zong Y. and Jin R. (2013). Structural mechanisms of the agrin-LRP4-MuSK signaling pathway in neuromuscular junction differentiation. Cell. Mol. Life Sci. 70, 3077-3088.

Accepted December 21, 2023